Appl Phys B (2010) 100: 903–908
DOI 10.1007/s00340-010-4167-7

Applied Physics B
Lasers and Optics

Propagation of general-type of phase-locked beam array in a turbulent atmosphere

P. Zhou · X. Wang · Y. Ma · H. Ma · X. Xu · Z. Liu

Received: 3 November 2009 / Revised version: 9 July 2010 / Published online: 8 August 2010

Abstract The propagation of a general-type of phase-locked beam array in a turbulent atmosphere is studied, in which four practical issues, i.e., apertured, conformal, partially coherent, and flattened beam array is taken into consideration for accurate modeling of beam array in power beaming applications. The average intensity distribution in the receiving plane is deduced analytically based on extended Huygens–Fresnel principle. The influence of beam order, transverse coherence length, and truncation ratio is briefly discussed.

1 Introduction

The phase-locked beam array has been under intense research recently because of its advantages and wide potential applications [1–10]. Characterizing the propagation properties of a high energy beam array offers good reference for evaluating the effect in practical environment. Gaussian beam array as a good approximation have been studied in detail to analysis the propagation properties of beam array in free-space or turbulent atmosphere [11–18]. Those phase-locked Gaussian beam arrays studied involve tiling an array of laser element with parallel optical axis closely together; each laser element is collimated and projected without apertures. The element beam spreads due to diffraction effect along the propagation range and there is constructive interference in the far-field. Nevertheless, the Gaussian beam array should be modified to present a more accurate model for power beaming in practical use thanks to the following four issues.

Firstly, a high-power laser element is often partially coherent, the linewidth is relatively large (several nm or even more) and the diffraction-limited transverse mode is not assured [18–22]. Secondly, the beam quality of a phase-locked Gaussian beam array suffers due to the low fill factor of Gaussian beamlets compared to fully filled, uniform (i.e., flat-top) near-field [2, 7, 9], this issue can be solved by shaping the near-field energy distribution of radiation from each element in laser array to be flattened beams [23–25]. Thirdly, each beam emitted from a laser system is more or less apertured [26–28]. Increasing the beam spot size to better fill the aperture will thus decrease the far-field energy spreading into side-lobes, but beyond a certain point will also cause increasing energy loss as the Gaussian beam is truncated by the finite-diameter aperture. Thereby the propagation properties of the beam array will be affected the truncation of the aperture, which should be taken into consideration in practice. Fourthly, the collimated beam projection with parallel optical axes will induce the average intensity at the receiving plane at a tactical range appears multi-laser-spots pattern (i.e. Fig. 3(a) in [11] and Fig. 2(a) in [12]), thus laser power is not mainly encircled in the central lobe, which is not expected for power beaming applications. In this way, the phase-locked beam array should be packed in a conformal configuration with each laser element radiated at the same target plane [29–31]. Taking the above-mentioned four issues into consideration, it is more exact to model the phase-locked beam array in practical engineering as an apertured conformal partially coherent flattened one.

To date, the propagation properties of partially coherent beam array [32–37], flattened beam array [38, 39], apertured beam array [40] and conformal beam array [31] in free-space or turbulent atmosphere has been studied in de-

P. Zhou · X. Wang · Y. Ma · H. Ma · X. Xu · Z. Liu (✉)
College of Optoelectric Science and Engineering,
National University of Defense Technology, Changsha 410073,
China
e-mail: zejinliu@vip.sina.com

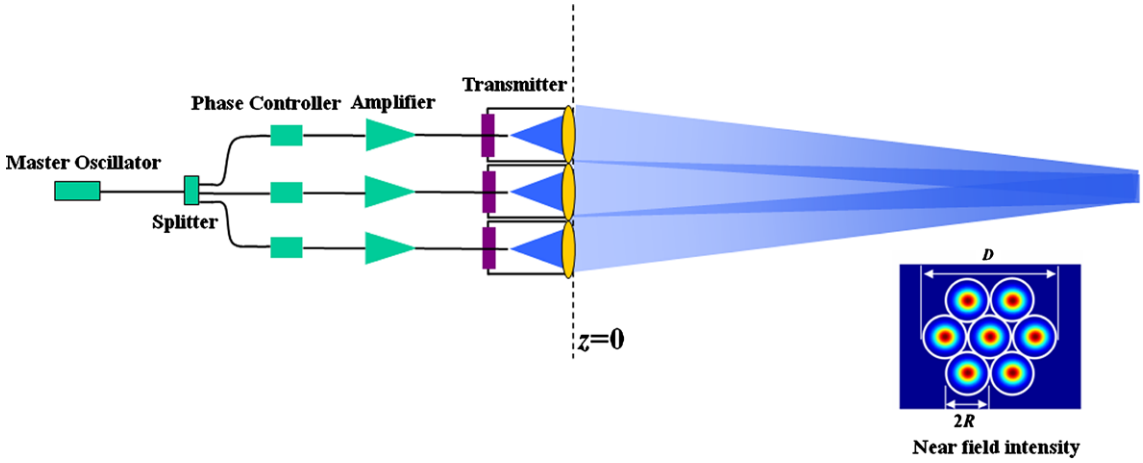

Fig. 1 Schematic diagram for phase-locked apertured conformal partially-coherent flattened beam array

tail respectively. Nevertheless, to the best of our knowledge, the more general case that includes all the issues that come up in practical power beaming applications, i.e., the propagation properties of a phase-locked apertured conformal partially coherent flattened beam array in a turbulent atmosphere has not yet been studied before. In the present paper, we will investigate the general propagation properties of a phase-locked apertured conformal partially coherent flattened beam array in a turbulent atmosphere, the averaged intensity distribution will be deduced analytically based on extended Huygens–Fresnel principle, and the effect of beam order, transverse coherence length, and truncation ratio on the laser power distribution in the receiving plane is evaluated in detail. Our motivation is to present an all-round computing and analyzing tool that offers some useful reference for fielding a phase-locked beam array in practical engineering.

2 Analysis of theory

The schematic diagram for projecting a phase-locked apertured conformal partially coherent flattened beam array into the target plane is shown in Fig. 1. The wavefront shape of each laser beam is tilted and projected onto a remote target simultaneously. Enclosed in Fig. 1 is the subfigure that indicates the near-field intensity distribution of the beam array truncated by an array of circular apertures with a radius of R. The whole diameter of the laser array D is defined by a circle of the smallest diameter that contains all the apertures.

We assume that the laser beam array is located at the source plane ($z = 0$). The field of each apertured tiled flattened laser beam element at the source plane can be expressed as [11–16, 31–36]

$$E_j(x, y, z = 0) = E_{j0}(x, y, 0) A_j(x, y, 0) \tag{1}$$

with

$$E_{j0}(x, y, 0) = \sum_{s=1}^{N} \frac{(-1)^{s-1}}{N} \binom{N}{s} \times \exp\{ik(x \sin\theta_{jx} + y \sin\theta_{jy})\} \times \exp\left\{-\frac{s[(x - a_j)^2 + (y - b_j)^2]}{\omega_0^2}\right\}, \tag{2}$$

$$A_j(x, y, 0) = \sum_{t=1}^{Q} B_t \exp\left\{-\frac{C_t}{R^2}[(x - a_j)^2 + (y - b_j)^2]\right\}, \tag{3}$$

where ω_0 denotes the width of the Gaussian distribution and (a_j, b_j) is the center of the j-th beamlet located at the source plane. To avoid multi-laser-spots pattern in the target plane in a collimated beam projection scheme with each beam direction parallel to each other, each laser beam is tilted projected to the same point in the target plane. We use $(\theta_{jx}, \theta_{jy})$ to denote the tilt angle in x and y directions of the j-th laser beam in the array, $\theta_{jx} = -a_j/L, \theta_{jy} = -b_j/L$. $k = 2\pi/\lambda$ is the wave number, λ is laser wavelength, L denotes the distance between the central of the source plane and the receiving plane along the propagation directions. $\binom{N}{n}$ denotes a binomial coefficient and N is the order of the flattened beams; a larger beam order corresponds to a more flattened beam shape. The flattened beam reduces to a Gaussian beam when $N = 1$. $A_j(x, y, 0)$ is the window function of hard-aperture that truncate the Gaussian beam and the complex constants B_t and C_t are the expansion coefficients that can be obtained by optimization computation directly [41, 42]. R denotes the radius of the sub-aperture that truncates the Gaussian beam. E_{j0} becomes a Gaussian beam without truncation when $N = 1$.

The complex degree of the spatial coherence for a partially beam can be expressed as [43]

$$g(x,y)=\frac{\sum_{u=1}^{N}\exp[-u(x^2+y^2)/2\Omega^2]}{N} \tag{4}$$

where Ω denotes the transverse coherence width of the laser beam, the degree of coherence between two points only depends on their position difference. The cross-spectral density of the whole beam array at the source plane can be written as [32–34, 44]

$$\begin{aligned}&W(x,y,\xi,\eta,0)\\&=\langle E(x,y,0)E^*(\xi,\eta,0)\rangle\\&=\sum_{j=1}^{M}\sum_{l=1}^{M}\sum_{u=1}^{N}E_j(x,y,0)E_l^*(\xi,\eta,0)\\&\quad\times\exp\{-u\{[(x-a_j)-(\xi-a_l)]^2\\&\quad+[(y-b_j)-(\eta-b_l)]^2\}/2\Omega^2\}/N,\end{aligned} \tag{5}$$

where (x,y) and (ξ,η) denotes the position coordinate at the $z=0$ plane. By using the extended Huygens–Fresnel principle, the average intensity of the conformal beam array after propagating in the turbulent atmosphere can be expressed as [45–47]

$$\begin{aligned}&\langle I(p,q,L)\rangle\\&=\frac{k^2}{(2\pi L)^2}\int_{-\infty}^{\infty}\int_{-\infty}^{\infty}\int_{-\infty}^{\infty}\int_{-\infty}^{\infty}W(x,y,\xi,\eta,0)\\&\quad\times\exp\left\{\frac{ik}{2L}[(p-x)^2+(q-y)^2-(p-\xi)^2\right.\\&\quad\left.-(q-\eta)^2]\right\}\langle\exp[\psi(x,y,p,q)\\&\quad+\psi^*(\xi,\eta,p,q)]\rangle dx\,dy\,d\xi\,d\eta,\end{aligned} \tag{6}$$

where (p,q) denotes the transverse coordinate at the receiving plane, $\psi(x,y,p,q)$ denotes the random part of the complex phase of a spherical wave that propagates from the source point to the receiving point, the angle brackets indicates the ensemble average over the medium statistics covering the log-amplitude and phase fluctuations due to the turbulent atmosphere. In this paper, the Kolmogorov spectrum and a quadratic approximation of the 5/3 power law for Rytov's phase structure function is employed [11]. The last term in the integrand of (4) can be written as [11–16, 31–36]

$$\begin{aligned}&\langle\exp[\psi(x,y,p,q)+\psi^*(\xi,\eta,p,q)]\rangle\\&=\exp\left\{-\frac{1}{\rho_0^2}[(x-\xi)^2+(y-\eta)^2]\right\}.\end{aligned} \tag{7}$$

Here $\rho_0=(0.545C_n^2k^2L)^{-3/5}$ is the coherence length of a spherical wave propagating in turbulent atmosphere with C_n^2 being the structure constant.

By combining (5)–(7), we can express the average intensity of the phase-locked apertured conformal partially coherent flattened beam array at the receiving plane in the following form

$$\begin{aligned}&\langle I(p,q,L)\rangle\\&=\frac{k^2}{(2\pi L)^2}\\&\quad\times\sum_{j=1}^{M}\sum_{l=1}^{M}\sum_{t=1}^{Q}\sum_{f=1}^{Q}\sum_{s=1}^{N}\sum_{h=1}^{N}\sum_{u=1}^{N}\Gamma_{j,l,t,f,s,h,u}(p,q,L),\end{aligned} \tag{8}$$

where

$$\begin{aligned}&\Gamma_{j,l,t,f,s,h,u}(p,q,L)\\&=\int_{-\infty}^{\infty}\int_{-\infty}^{\infty}\int_{-\infty}^{\infty}\int_{-\infty}^{\infty}\frac{(-1)^{s+h}B_tB_h^*}{N^3}\binom{N}{s}\binom{N}{h}\\&\quad\times\exp\left\{-\frac{s[(x-a_j)^2+(y-b_j)^2]}{\omega_0^2}\right\}\\&\quad\times\exp[ik(x\sin\theta_{jx}+y\sin\theta_{jy})]\\&\quad\times\exp\left\{-\frac{h[(\xi-a_l)^2+(\eta-b_l)^2]}{\omega_0^2}\right\}\\&\quad\times\exp[-ik(\xi\sin\theta_{l\xi}+\eta\sin\theta_{l\eta})]\\&\quad\times\exp\left\{-\frac{C_t[(x-a_j)^2+(y-b_j)^2]}{R^2}\right\}\\&\quad\times\exp\left\{-\frac{C_h^*[(\xi-a_l)^2+(\eta-b_l)^2]}{R^2}\right\}\\&\quad\times\exp\left\{-\frac{u[(x-a_j)-(\xi-a_l)]^2}{2\Omega^2}\right.\\&\quad\left.-\frac{u[(y-b_j)-(\eta-b_l)]^2}{2\Omega^2}\right\}\\&\quad\times\exp\left\{\frac{ik}{2L}[(p-x)^2+(q-y)^2\right.\\&\quad\left.-(p-\xi)^2-(q-\eta)^2]\right\}\\&\quad\times\exp\left\{-\frac{1}{\rho_0^2}[(x-\xi)^2+(y-\eta)^2]\right\}dx\,dy\,d\xi\,d\eta.\end{aligned} \tag{9}$$

The deduction process for (9) is tedious but straightforward; by using the integral formula (3.323.2) in Ref. [48]

and performing the related integral in (9) we can obtain

$$\Gamma_{j,l,s,h,t,f,u}(p,q,L) = \frac{B_t B_f^* \pi^2}{\gamma_1 \gamma_2} \frac{(-1)^{s+h}}{N^3} \binom{N}{s} \binom{N}{h} \times H(p,L) H(q,L), \tag{10}$$

where

$$H(p,L) = \exp\left\{-\frac{a_j^2}{\omega_{s,t}^2} - \frac{a_l^2}{\omega_{h,f}^2} - \frac{(a_j - a_l)^2}{2\Omega^2}\right\} \times \exp\left\{\frac{\beta_{1x}^2}{4\gamma_1} + \frac{\beta_{2x}^2}{4\gamma_2}\right\}. \tag{11a}$$

$$H(q,L) = \exp\left\{-\frac{b_j^2}{\omega_{s,t}^2} - \frac{b_l^2}{\omega_{h,f}^2} - \frac{(b_j - b_l)^2}{2\Omega^2}\right\} \times \exp\left\{\frac{\beta_{1y}^2}{4\gamma_1} + \frac{\beta_{2y}^2}{4\gamma_2}\right\}. \tag{11b}$$

$$\frac{1}{\omega_{s,t}^2} = \frac{s^2}{\omega_0^2} + \frac{C_t}{R^2}, \tag{11c}$$

$$\frac{1}{\omega_{h,f}^2} = \frac{h^2}{\omega_0^2} + \frac{C_f^*}{R^2}, \tag{11d}$$

$$\gamma_1 = \frac{1}{\omega_{s,t}^2} + \frac{1}{\rho_1^2}, \tag{11e}$$

$$\gamma_2 = \frac{1}{\omega_{h,f}^2} + \frac{1}{\rho_1^2} - \frac{1}{\rho_1^4 \gamma_1}, \tag{11f}$$

$$\beta_{1x} = \frac{2a_j}{\omega_{s,t}^2} - ik\sin\theta_{jx} + \frac{ikp}{L} + \frac{u(a_j - a_l)}{\Omega^2}, \tag{11g}$$

$$\beta_{1y} = \frac{2b_j}{\omega_{s,t}^2} - ik\sin\theta_{jy} + \frac{ikq}{L} + \frac{u(b_j - b_l)}{\Omega^2}, \tag{11h}$$

$$\beta_{2x} = \frac{2a_l}{\omega_{h,f}^2} + ik\sin\theta_{l\xi} - \frac{ikp}{L} + \frac{\beta_{1x}}{\rho_1^2 \gamma_1} + \frac{u(a_j - a_l)}{\Omega^2}, \tag{11i}$$

$$\beta_{2y} = \frac{2b_l}{\omega_{h,f}^2} + ik\sin\theta_{l\eta} - \frac{ikq}{L} + \frac{\beta_{1y}}{\rho_1^2 \gamma_1} + \frac{u(b_j - b_l)}{\Omega^2}, \tag{11j}$$

$$\rho_1^2 = \frac{2\rho_0^2 \Omega^2}{2\Omega^2 + u\rho_0^2}. \tag{11k}$$

Equations (10)–(11) are the main analytical result of the present paper, which can be used for studying the propagating properties of a phase-locked apertured conformal partially coherent flattened beam array in the turbulent atmosphere.

3 Numerical calculating and analysis

In this section, we perform some numerical calculations as an example to illustrate the propagation properties of conformal beam array in atmospheric turbulence. To see the propagation properties, we calculate the intensity profile on the receiving plane for a 7-laser array packaged as shown in Fig. 1. Figure 2 shows intensity distribution in the receiving plane for the beam array with different transverse coherence width propagating at a distance of $L = 5$ km. The laser parameters used are set as follows: $\lambda = 1.06$ μm, $\omega_0 = d/2 = 1$ cm, $R = 1.5$ cm, $D = 9$ cm, $N = 4$. The structure constant of the turbulent atmosphere is set to be $C_n^2 = 10^{-15}\mathrm{m}^{-2/3}$. It is seen that the laser power is more encircled in the central lobe as an increase in the transverse coherence width.

Figure 3 shows intensity distribution in the receiving plane for the beam array with different truncation ratio propagating at a distance of $L = 5$ km, the transverse coherence is chosen to be $\Omega = 10\omega_0$. The truncation factor is defined as $F_\mathrm{t} = R/\omega_0$; smaller F_t corresponds to more energy being clipped by the apertures. It is to be seen that smaller F_t makes more laser power encircled in the central lobe because an outgoing beamlet with a more uniform intensity distribution is obtained. This conclusion is consistent with the Gaussian beam array propagating in free-space [29]. Nevertheless, decreasing F_t beyond a certain point will also cause increased power loss. Thus a tradeoff should be performed between the energy loss due to beam truncating and improvement in power concentrating according to the practical array parameters.

Figure 4 shows intensity distribution in the receiving plane for the beam array with different beam orders propagating at a distance of $L = 10$ km, the transverse coherence is chosen to be $\Omega = 2\omega_0$. The other parameters of the laser array are kept the same with those used in Fig. 2. It is found that power focusability of beam array with higher order is better than its lower order counterparts because less laser power will be contained in the side-lobes.

Figure 5 shows intensity distribution in the receiving plane for the beam array propagating with distance of $L =$ 10 km, 20 km and 100 km, the transverse coherence is $\Omega = 2\omega_0$. The other parameters of the laser array are kept the same with those used in Fig. 2. It is seen that at a short propagation distance (corresponds to a large coherence length), the laser intensity pattern is non-Gaussian shape with multiple side-lobes. The irradiance distribution profiles for coherent combined beams evolves from typical non-Gaussian with multiple side-lobes into Gaussian shape with the coherence length decreasing, which is caused by the isotropic influence of the atmosphere turbulence [11].

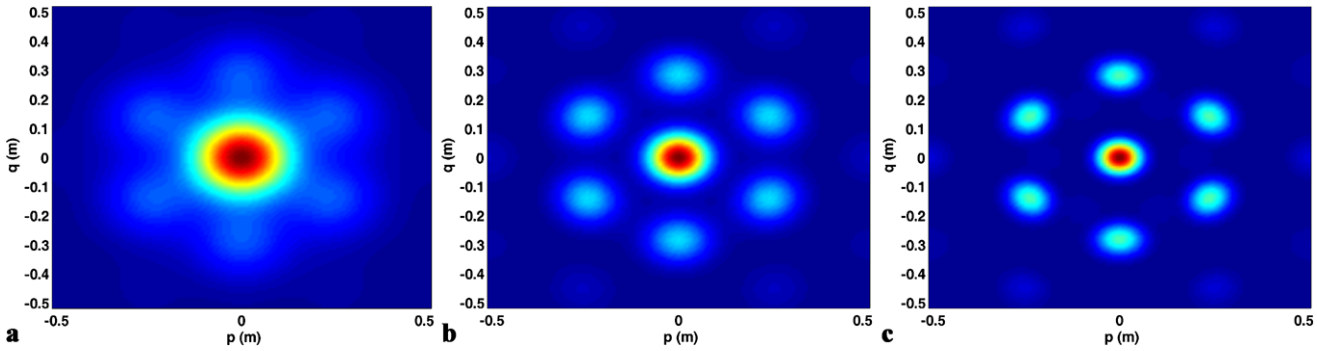

Fig. 2 Intensity distributions for beam array with different transverse coherence (**a**) $\Omega = \omega_0$, (**b**) $\Omega = 2\omega_0$, (**c**) $\Omega = 10\omega_0$

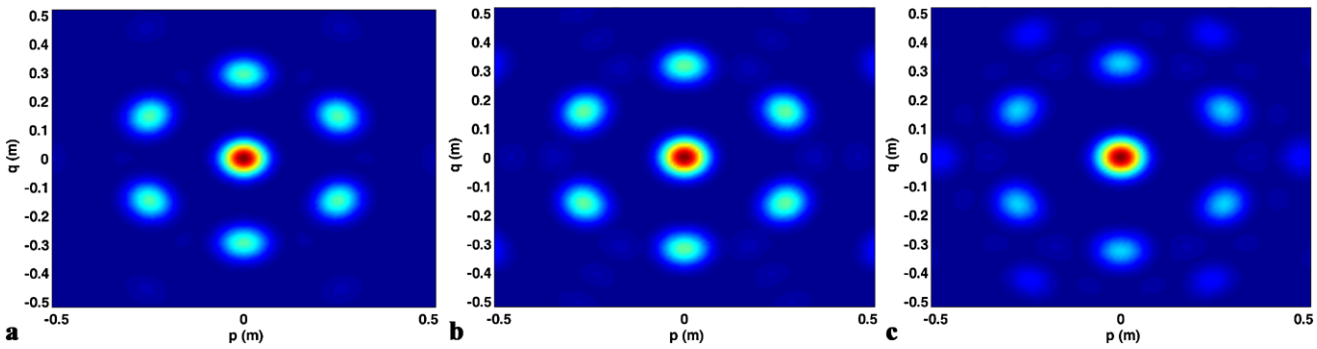

Fig. 3 Intensity distributions for beam array with different truncation ratio (**a**) $R = 0.8\omega_0$, (**b**) $R = \omega_0$, (**c**) $R = 1.2\omega_0$

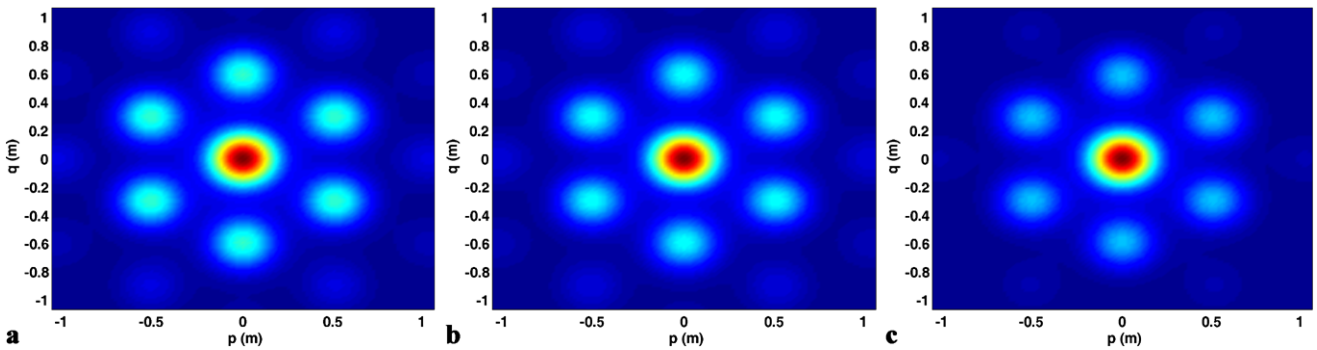

Fig. 4 Intensity distribution for beam array with different beam orders (**a**) $N = 1$, (**b**) $N = 3$, (**c**) $N = 5$

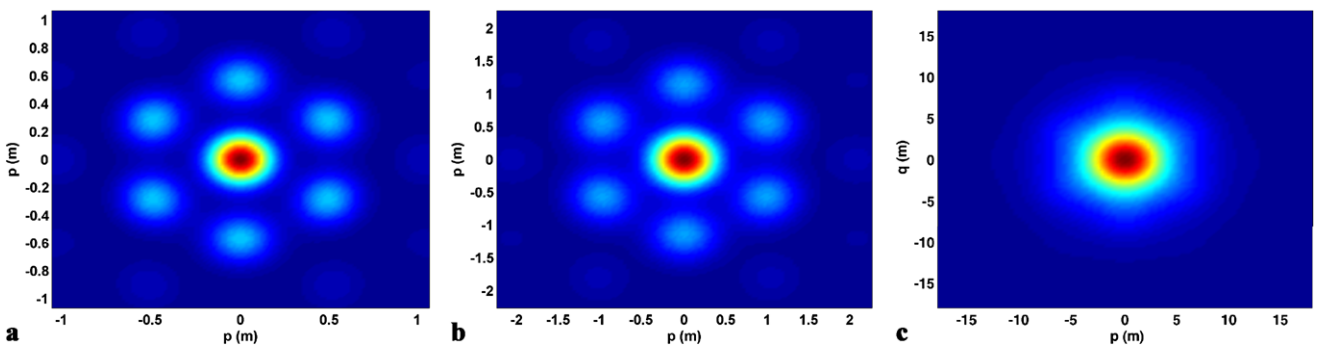

Fig. 5 Intensity distribution for beam array with different propagating distance (**a**) $L = 10$ km, (**b**) $L = 20$ km, (**c**) $L = 100$ km

4 Conclusions

We have taken four practical issues into consideration for accurate modeling of a general-type of phase-locked beam array, and derived uniform analytical formulae for the propagation properties of beam array in a turbulent atmosphere based on extended Huygens–Fresnel principle. The effect of beam order, transverse coherence length, and truncation ratio is discussed in detail. It is concluded that more laser power is contained in the central lobe with an increase in the transverse coherence width and beam orders, and the truncation ratio should be properly selected in tradeoff between the energy loss due to beam truncating and improvement in power concentrating. The conclusions in this paper represent a good reference for analyzing and designing a phase-locked array power beaming system.

Acknowledgement This work is supported by Hunan Provincial Innovation Foundation for Postgraduates.

References

1. A. Desfarges-Berthelemot, V. Kermène, D. Sabourdy, J. Boullet, P. Roy, J. Lhermite, A. Barthélémy, C. R. Phys. **7**, 244 (2006)
2. T.Y. Fan, IEEE J. Sel. Top. Quantum Electron **11**, 567 (2005)
3. C.J. Corcoran, F. Durville, Appl. Phys. Lett. **86**, 201118 (2005)
4. P. Zhou, Z. Liu, X. Wang, Y. Ma, H. Ma, X. Xu, S. Guo, Appl. Phys. Lett. **94**, 231106 (2009)
5. W. Liang, N. Satyan, F. Aflatouni, A. Yariv, A. Kewitsch, G. Rakuljic, H. Hashemi, J. Opt. Soc. Am. B **24**, 2930 (2007)
6. T.M. Shay, J.T. Baker, Anthony D. Sanchez, C.A. Robin, L.C.L. Vergien, C. Zerinque, A.D. Sanchez, D. Gallant, C.A. Lu, B. Pulford, C.T.J. Bronder, A. Lucero, Proc. SPIE **7195**, 71951M (2009)
7. J. Anderegg, S. Brosnan, E.C. Cheung, P. Epp, D. Hammons, H. Komine, M. Weber, M. Wickham, Proc. SPIE **6102**, 61020U (2006)
8. S.J. Augst, J. Ranka, T.Y. Fan, A. Sanchez, J. Opt. Soc. Am. B **24**, 1707 (2007)
9. G.D. Goodno, C.P. Asman, J. Anderegg, S. Brosnan, E.C. Cheung, D. Hammons, H. Injeyan, H. Komine, W.H. Long Jr., M. McClellan, S.J. McNaught, S. Redmond, R. Simpson, J. Sollee, M. Weber, S. Benjamin Weiss, M. Wickham, IEEE J. Sel. Topics Quantum Electron. **13**, 460 (2007)
10. J.E. Kansky, C.X. Yu, D.V. Murphy, S.E.J. Shaw, R.C. Lawrence, C. Higgs, Proc. SPIE **6306**, 63060G (2006)
11. Y. Cai, Y. Chen, H.T. Eyyuboğlu, Y. Baykal, Appl. Phys. B **88**, 467 (2007)
12. X. Chu, Z. Liu, Y. Wu, J. Opt. Soc. Am. A **25**, 74 (2008)
13. H.T. Eyyuboğlu, Y. Baykal, Y. Cai, Appl. Phys. B **91**, 265 (2008)
14. X. Ji, X. Li, Acta Phys. Sin. **57**, 7674 (2008)
15. P. Zhou, Z. Liu, X. Xu, X. Chu, Opt. Commun. **282**, 1640 (2009)
16. X. Ji, X. Li, J. Opt. Soc. Am. A **26**, 236 (2009)
17. B. Lü, H. Ma, Opt. Commun. **171**, 185 (1999)
18. http://www.strommedia.us/25/2542/A254254.html
19. Y. Jeong, J.K. Sahu, D.N. Payne, J. Nilsson, Opt. Express **12**, 6088 (2004)
20. http://www.ipgphotonics.com/Collateral/Documents/English_US/HP_Broshure.pdf
21. S. Norman, M. Zervas, A. Appleyard, M. Durkin, R. Horley, M. Varnham, J. Nilsson, Y. Jeong, Proc. SPIE **5335**, 229 (2004)
22. X. Li, X. Chen, X. Ji, Opt. Commun. **282**, 7 (2009)
23. S.J. Brosnan, M.G. Wichham, H. Komine, US patent 72283702, 2007
24. Y. Cai, Q. Lin, J. Opt. A, Pure Appl. Opt. **6**, 390 (2004)
25. Y. Cai, J. Opt. A, Pure Appl. Opt. **8**, 537 (2006)
26. H.T. Yura, Appl. Opt. **34**, 2774 (1995)
27. X. Chu, Y. Ni, G. Zhou, Opt. Commun. **274**, 274 (2007)
28. X. Ji, G. Ji, J. Opt. Soc. Am. A **25**, 1246 (2008)
29. M.A. Vorontsov, S.L. Lachinova, J. Opt. Soc. Am. A **25**, 1949 (2008)
30. M.A. Vorontsov, T. Weyrauch, L.A. Beresnev, G.W. Carhart, L. Liu, K. Aschenbach, IEEE J. Sel. Top. Quantum Electron. **15**, 269 (2009)
31. P. Zhou, X. Wang, Y. Ma, H. Ma, X. Xu, Z. Liu, J. Opt. A, Pure Appl. Opt. **11**, 105707 (2009)
32. X. Ji, E. Zhang, B. Lü, J. Opt. Soc. Am. B **25**, 825 (2008)
33. Y. Cai, Q. Lin, H.T. Eyyuboğlu, Y. Baykal, Opt. Commun. **278**, 157 (2007)
34. Y. Zhu, D. Zhao, X. Du, Opt. Express **16**, 18437 (2008)
35. E. Zhang, X. Ji, B. Lü, Chin. Phys. B **18**, 571 (2008)
36. X. Ji, X. Chen, B. Lü, J. Opt. Soc. Am. A **25**, 21 (2008)
37. B. Li, B. Lü, J. Opt. A, Pure Appl. Opt. **5**, 303 (2003)
38. G. Wu, Q. Lou, J. Zhou, J. Dong, Y. Wei, Opt. Laser Technol. **40**, 890 (2008)
39. P. Zhou, Z. Liu, X. Xu, X. Chu, Opt. Laser. Eng. **47**, 1254 (2009)
40. S.L. Lachinova, M.A. Vorontsov, J. Opt. Soc. Am. A **25**, 2008 (1960–1973)
41. Y. Zhang, Opt. Commun. **248**, 317 (2005)
42. J.J. Wen, M.A. Breazeale, J. Acoust. Soc. Am. **83**, 1752 (1988)
43. G. Wu, H. Guo, D. Deng, Appl. Opt. **45**, 366 (2006)
44. X. Xiao, X. Ji, B. Lü, Opt. Laser Technol. **40**, 129 (2008)
45. L.C. Andrews, R.L. Phillips, *Laser Beam Propagation through Random Media* (SPIE Press, Bellingham, 1998)
46. H.T. Eyyuboğlu, Y. Baykal, Opt. Express **12**, 4659 (2004)
47. S.C.H. Wang, M.A. Plonus, J. Opt. Soc. Am. **69**, 1297 (1979)
48. I.S. Gradshteyn, I.M. Ryzhik, *Tables of Integrals, Series and Products* (Academic Press, New York, 1980)